Editorial Manager(tm) for Bulletin of Earthquake Engineering
Manuscript Draft

Manuscript Number: BEEE496R1

Title: Identification of accelerometric stations in ITACA with distinctive features in their seismic response

Article Type: SI: Italian strong motion database ITACA

Keywords: Strong motion; inter-station; Italy; site classification

Corresponding Author: Dino Bindi, PhD

Corresponding Author's Institution: Istituto Nazionale di Geofisica e Vulcanologia

First Author: Dino Bindi, PhD

Order of Authors: Dino Bindi, PhD;Lucia Luzi;Francesca Pacor;Roberto Paolucci

Abstract: In this work, we analyze the records of the Italian strong motion database (ITACA, http://itaca.mi.ingv.it) with the aim of identifying stations affected by site effects that are not captured by standard seismic classification schemes. In particular, we consider four different site classifications, two of them based on geological/geophysical characteristics and two driven by data. For each classification we develop a ground motion prediction equation using a random effect approach to isolate the between-station and within-station distribution of errors. The site coefficients obtained for the different classes confirm that site amplification effects are significant for both the horizontal and vertical components. The between-station error normalized to the standard deviation of the between-station error distribution is then used to identify stations characterized by large errors, attributable to site effects not accounted for by the classification schemes. The results show that large errors can affect the predictions when the site effects are not uniquely related to the reduction of the seismic impedance in the uppermost layers. For example, amplifications of ground motion over the long period range are observed for stations installed within alluvial closed-shape basins, as consequence of locally generated surface waves. For these stations, classifications based on the horizontal to vertical response spectra ratio are not reliable, since amplifications are also affecting the vertical component. Another interesting feature which emerges from the analysis is the significant de-amplification of short period spectral ordinates that seems to be related to stations typically set in at the foundation level of massive structures. To increase the usefulness of the data set, the most important distinctive features of the strong motion stations are documented in the ITACA database reports containing the instrument information and the available geological-geotechnical data.

Response to Reviewers: Our responses to the questions raised by reviewers are attached as files.

Identification of accelerometric stations in ITACA with distinctive features in their seismic response

Dino Bindi[1,2], Lucia Luzi[2], Francesca Pacor[2], Roberto Paolucci[3]

[1] GFZ German Research Centre for Geosciences and CEDIM, Potsdam, Germany
[2] Istituto Nazionale di Geofisica e Vulcanologia, Milano, Italy
[3] Department of Structural Engineering, Politecnico di Milano, Italy

Abstract

In this work, we analyze the records of the Italian strong motion database (ITACA, http://itaca.mi.ingv.it) with the aim of identifying stations affected by site effects that are not captured by standard seismic classification schemes. In particular, we consider four different site classifications, two of them based on geological/geophysical characteristics and two driven by data. For each classification we develop a ground motion prediction equation using a random effect approach to isolate the between-station and within-station distribution of errors. The site coefficients obtained for the different classes confirm that site amplification effects are significant for both the horizontal and vertical components. The between-station error normalized to the standard deviation of the between-station error distribution is then used to identify stations characterized by large errors, attributable to site effects not accounted for by the classification schemes. The results show that large errors can affect the predictions when the site effects are not uniquely related to the reduction of the seismic impedance in the uppermost layers. For example, amplifications of ground motion over the long period range are observed for stations installed within alluvial closed-shape basins, as consequence of locally generated surface waves. For these stations, classifications based on the horizontal to vertical response spectra ratio are not reliable, since amplifications are also affecting the vertical component. Another interesting feature which emerges from the analysis is the significant de-amplification of short period spectral ordinates that seems to be related to stations typically set in at the foundation level of massive structures. To increase the usefulness of the data set, the most important distinctive features of the strong motion stations are documented in the ITACA database reports containing the instrument information and the available geological-geotechnical data.

1 Introduction

The prediction of ground motion amplitude, generated by an earthquake of given magnitude occurring at a given distance form the site of interest, is an important task for engineering seismology and seismic hazard oriented studies. This task is generally accomplished by considering models, called Ground Motion Prediction Equations (GMPEs), calibrated through regressions, applied to strong-motion data recorded from past earthquakes (Douglas, 2003). Besides the prediction of the expected median value, the statistical uncertainty affecting the median is also playing an important role in assessing the seismic hazard. This uncertainty arises from the intrinsic ground motion variability that cannot be fully captured by any regression model. Furthermore, since the actual ground motion results from the interaction of complex phenomena, related to the generation and propagation of seismic waves, several simplifications are introduced in selecting a suitable model for developing the GMPEs. As a result, both aleatory and epistemic uncertainties affect the predictions (Toro et al., 1997; Strasser et al.; 2009; Al Atik et al., 2010).

Among many other factors, the characteristic of the subsurface geology can play an important role in determining the level of ground shaking, as well as its spatial variability. In general, the GMPEs account for site amplification effects through simplified approaches, such as the introduction of site classes or site parameters as proxies for local site effects, e.g. the shear wave velocity averaged over the uppermost 30 m (V_{s30}). Although the introduction of either site classes or a continuous function of V_{s30} is an attempt to model the average effect of local amplifications, it cannot capture the large variability affecting the site responses of stations belonging to the same class or having the same V_{s30} (e.g. Bragato, 2008; 2009).

In the framework of Project S4 (http://esse4.mi.ingv.it), that has accomplished the development of the new Italian strong motion database ITACA (ITalian ACelerometric Archive, http://itaca.mi.ingv.it), several investigations, such as (a) geomorphology study (Di Capua et al., 2011); (b) station-structure interaction effects (Mucciarelli, 2010) ; (c) in-field monitoring activity (Bindi et al., 2011; Cara et al., 2011; Massa et al., 2010); (d) numerical modelling (Lovati et al., 2011; Smerzini et al., 2011), were performed to clarify to which extent the records in ITACA may show systematic bias related to characteristics of the recording site. In this work, we will refer to stations showing distinctive features, i.e., those stations whose predictions systematically either under or over-estimate the median predictions computed for the site class they belong to.

The identification of a subset of ITACA stations, for which such features are apparent, is expected to improve the quality of the available information in the dataset. For instance, the identification of stations lying in closed-shaped alluvial basin will make more rationale the selection of accelerograms in similar geological conditions for engineering applications. Similarly, the end-user should be aware of records which are obtained at a rock outcrop where the topography or the lateral geological heterogeneities may strongly affect the seismic response. As a matter of a fact, researchers and professionals, who access a strong motion database to download strong-motion records satisfying prescribed criteria, in most cases are not aware of the actual recording conditions and merely rely upon the available, often qualitative, seismic classification of the site. Therefore, although the selection meets the target magnitude, such as distance and site classification, the accelerograms may not be suitable for the engineering or seismic hazard applications they were selected for, because their peak values or spectral content can be affected by complex source, path or site effects. It follows that the identification of such stations and the description of their distinctive features in the station monograph, can substantially improve the quality of the database.

This article is organized as follows. We first derive a set of GMPEs for spectral accelerations, considering four different site classification schemes. For each scheme, the residuals between observations and predictions are computed and the between-station contribution (corresponding to the site-to-site variability as defined in Al Atik et al., 2010) isolated by considering a random effect model (Abrahamson and Youngs, 1992). Finally, stations showing distinctive features are identified by analyzing the between-station distribution of error normalized to its standard deviation and possible causes of the observed systematic over or underestimations are discussed.

2. Between-station error distribution

When observations and predictions are compared, systematic over or under-estimations may be observed because of several causes, such as: i) geological and/or morphological conditions that may cause ground motion amplification or de-amplification in certain period ranges, usually not accounted for in standard site classification schemes; ii) earthquake source and directivity effects, high/low stress drops, shallow/deep hypocenters, which may lead to ground motions amplitudes significantly beyond/below the standard dispersion bands for a group of records; iii) the interaction between the recording stations and the hosting or nearby structures.

Independently from the cause, these features can be detected by analyzing the average residuals of several records at the same station, or records of the same earthquake at several stations.

Figure 1 shows the comparison between the spectral acceleration, predicted by a GMPE derived for Italy (Bindi et al., 2010) and the observations of the same earthquake recorded at different stations (left), or several earthquakes recorded at the same station (right). On the left panel the spectral accelerations at 0.1s, predicted for a magnitude 4.25 earthquake (black curve), are compared to the observations of a magnitude 4.3 earthquake occurred on 2002/11/04 (red circles) and a magnitude 4.2 earthquake occurred on 1997/10/07 (blue circles). The positive (blue) and negative (red) between-event errors obtained for the two earthquakes indicate that, on average, the predictions under- and over-estimate the observations, respectively. Similarly, in the right panel, the spectral acceleration at 1.75 s, predicted for a magnitude 5.5 earthquake, systematically under-estimate the observations at the GBP site (red) and over-estimate those at CLC (blue), while the average error for the AVZ (green) site is almost zero.

Since we aim at identifying the stations showing distinctive features (such as GBP and CLC in Figure 1), in this study the regressions to calibrate the GMPEs are performed by applying a random effect approach (e.g., Abrahamson and Youngs, 1992) but separating the between-station and within-station components (e.g. Bindi et al., 2006), that is:

$$r_{i,j} = \varepsilon_i + \eta_{i,j} \quad (1)$$

where $r_{i,j,}$ is the residual (difference between the logarithm of observation and prediction) relevant to earthquake j recorded at station i, ε is the between-station (or inter-station) and η the within-station (or intra-station) error, as shown in the left panel of Figure 1. The terminology between-station and within-station is derived by analogy with the between-event and within-event terminology introduce by Al Atik et al. (2010). The two error distributions are assumed to be independent and normally distributed, with between-station standard deviation τ and within-station standard deviation ϕ, respectively (e.g., Bindi et al.; 2006; Bindi et al.; 2009a). The total standard deviation σ, associated to median prediction from model (1), is $\sigma = \sqrt{\tau^2 + \phi^2}$. It is worth remembering that in model (1) the between-event component of variability, describing the average residuals for different records of the same earthquake, as shown in the left panel of Figure 1, is part of the within-station component of error.

3. Data set

The strong-motion data used to derive the GMPEs are retrieved from the ITACA strong motion database (Luzi et al., 2008), and have been classified using four different site classification schemes, described in Table 1. The first scheme, hereinafter referred to as SP, is composed by three classes identified mainly by geological characteristics (Sabetta and Pugliese, 1987, 1996). It separates rock sites (class 0) from soil sites, where the soil sites are in turn divided into shallow alluvium (class 1) and deep alluvium (class 2), depending on a threshold sediment depth of 20 m. The second classification scheme, hereinafter referred to as EC8, is the one introduced by Eurocode8 (CEN, 2004). EC8 discriminates 5 main classes, A through E, based on intervals of the shear wave velocity averaged over the uppermost 30m (V_{s30}), as described in Table 1. For defining class E, the depth of the sediments is also considered. It is worth to specify that about 100 stations in ITACA have an in-site measured shear-wave velocity profile. For the rest of the stations the EC8 class was inferred mainly on the base of geological information.

The other two schemes are data driven and are based on the ratio between the horizontal and vertical acceleration response spectra (5% damping), HVRS. In particular, after Zhao et al (2006), Di Alessandro et al (2008) introduced a classification, hereinafter referred to as DiAlAl, based on the site predominant period (Table 1). Luzi et al (2011) proposed a site classification, hereinafter referred to as LuAl, including 5 classes, F-0 through F-4, based on the site fundamental frequency (Table 1). The regressions are performed considering different data sets, since the information is not sufficient to classify all stations accordingly to the four different schemes.

The number of stations, earthquakes and recordings, used to develop the GMPEs for the different classification schemes are listed in Table2. The selected records, for all the adopted classification schemes, span the magnitude range 3.5-6.9 and the maximum distance is 300 km, as shown in Figure 2.

4. Evaluation of GMPEs

A set of GMPEs has been developed considering the four site classification schemes, previously described. The functional form for predicting the median ground motion is a simplified version of the Boore and Atkinson's (2008). In particular, since the maximum magnitude of the analyzed data set is 6.9, we do not introduce the hinge magnitude and we do not include terms describing the non-linear soil behaviour. The functional form is the following:

$$\log_{10} Y = e_1 + F_D(R,M) + F_M(M) + F_S + F_{sof} \quad (2)$$

where e_1 is the constant term, F_D(R, M), F_M (M), F_s and F_{sof} represent the distance function, the magnitude scaling, the site amplification and the style of faulting correction, respectively. M is the moment magnitude or the local magnitude for weak events (M < 4.5), R is the Joyner-Boore distance or the epicentral distance (in km) when the fault geometry is unknown (generally when M < 5.5).

The strong motion parameter Y considered for the regressions is the 5% damping acceleration response spectra (Sa, cm/s^2), considering 23 periods from 0.04 s to 4 s. The proposed equation for the distance function is:

$$F_D(R,M) = \left[c_1 + c_2\left(M - M_{ref}\right)\right]\log_{10}\left(\sqrt{R_{JB}^2 + h^2} / R_{ref}\right) + c_3\left(\sqrt{R_{JB}^2 + h^2} - R_{ref}\right) \quad (3)$$

whereas the magnitude function is:

$$F_M(M) = b_1\left(M - M_{ref}\right) + b_2\left(M - M_{ref}\right)^2 \quad (4)$$

where M_{ref} =5 and R_{ref} =1 km.

The functional form F_S in equation (2) represents the site amplification and it is given by $F_S = s_j C_j$, for j=1,...$N_{classes}$, where s_j are the coefficients to be determined through the regression analysis, and C_j are dummy variables used to denote the different site classes (Table 1). The functional form F_{sof} represents the style of faulting correction and it is given by $F_{sof} = f_j E_j$, for j=1,...4, where f_j are the coefficients to be determined during the analysis and E_j are dummy variables used to denote the different fault classes. We considered 4 types of style of faulting: normal (N), reverse (R), strike slip (SS) and unknown (U). The distributions of the analyzed records for different site classes are shown in Figure 2. In performing the regressions, the rock site coefficients, i.e. classes 0 (SP), A (EC8), F-0 (LuAl), CL-V (DiAAl), are constrained to zero and used as reference for the other site coefficients. We also constrained to zero the style of faulting coefficient of the unknown class (f_4), as well as the average of the style of faulting coefficients ($f_1 + f_2 + f_3 = 0$). The regressions are performed considering the geometrical mean of the recorded horizontal (hereinafter GeoH) and the vertical components (hereinafter Z).

Before discussing the results we remind that the aim of this work is to debate the distribution of residuals, obtained considering different site classification schemes, and not to provide alternative GMPEs to be used for the Italian territory.

4.1 Site coefficients

In equation (2), the site coefficients s_j quantify the period dependent average amplification for each considered site class (j=1,…,N, where N is number of classes), with respect to a reference class. The site coefficients as a function of the period, obtained for the four classification schemes, are shown in Figures 3a (GeoH) and 3b (Z).

For the GeoH component, large site terms are found for all classification schemes. Amplifications at long periods, peaked at about 1 s, occur for classes 2 (SP), class D (EC8), class F-1 (LuAl), and CL-IV (DiAlAl). Most stations installed in alluvial basins belong to these classes.

Furthermore, class E (EC8) and class F-3 (LuAl) show amplifications larger than 0.6 over the short period range, with a maximum amplification at 0.1 s. These classes include few stations and, in particular, the stations co-located in Nocera Umbra (i.e. NCR and NCR2), which are stations with a considerable number of recordings in the ITACA database. Therefore, the site coefficients for classes E and F-3 are representative of the strong amplification occurring at this site (Rovelli et al.; 2002; Cultrera et al. 2003; Castro et al., 2004). Finally, classes F-2 through F-3 (LuAl), as well as classes CL-I through CL-IV (DiAlAl), show coefficients larger than 0.4, with peaks centered at periods shorter than 0.3s, in agreement with the boundaries used to define each class.

The site amplifications affecting the vertical component are also not negligible, as shown in Figure 3b. In particular, for stations installed within alluvial basins (e.g. F-1 and CL-IV) large amplifications over a broad range of periods (0.6s – 2s) are predicted. It is worth noting that, when sites show amplification at long periods (e.g. class D of EC8), the maximum values for the vertical component occur at periods shorter than the horizontal ones, as in theory and in agreement with the empirical results obtained for several alluvial basins in Central Italy (Castro et a.; 2004; Luzi et al.; 2005), where 2D-3D site effects related to locally generated surface waves have been identified.

5. Analysis of between-station residuals

Figure 4 shows an example of between-station residuals ε for the GeoH component obtained at four different periods, 0.1s (top left), 0.25s (top right), 1s (bottom left) and 2s (bottom right), considering the data set classified according to the EC8 scheme.

Large dispersion of the between-station residuals are observed for classes A (red) and B (orange) in the short to medium period range (top). The seismic response of stations classified as rock or stiff sites may be typically modified by topographic effects, thin weathered rock layers or soil-structure interaction. A well known example of such stations is Tolmezzo-Ambiesta, TLM, classified as rock. The TLM record of the M 6.4, 1976 Friuli earthquake has been largely used to calibrate attenuation relationships in Italy and Europe (Ambraseys et al., 2004) and as an input for structural analyses and/or site amplification studies. Barnaba et al (2007) demonstrated that the high amplification observed at this station can be attributed to the interaction with the Ambiesta dam, being the station located above the abutment.
Class B sites, characterized by Vs30 ranging from 360 to 800 m/s, have a seismic response that may be amplified over quite different frequency ranges as exemplified by stations AQK and AQV, which recorded the 2009 L'Aquila seismic sequence. Although these sites are both classified as B, they show the largest amplification peak at very different frequencies, 1.6 s and 0.3s, respectively.

At longer periods (Figure 4, bottom), the dispersion of classes A and B decreases, while several class C (cyan curve) stations show large positive errors (under-estimation). Most of them are installed in alluvial basins (e.g GBP, Gubbio Piana; BTT2, Borgo Ottomila; RTI, Rieti) and their recordings are strongly contaminated by locally generated surface waves.

In the following, we illustrate how the between-station error distributions for specific stations can be used to infer the site response and the reliability of the assigned site category. The results are discussed in terms of between-station error ε normalized to τ, to quantify the misfit with the median prediction as number of standard deviations. Four sites, belonging to different classes, are shown as example in Figure 5, for the mean horizontal (left) and vertical (right) components.

The between-station residuals at Gubbio Piana (GBP, triangle, class C) and Rieti (RTI, circle, class D), both located within close-shaped alluvial basins, indicate that predictions strongly under estimate (normalized residuals close to or larger than 2) the observations at periods longer than 1 s, accordingly to previous studies (e.g. Ambraseys et al., 2005). The case of station GBP is well known as it has been the subject of several studies (e.g., Pacor et al., 2007; Bindi et al., 2009b; Smerzini et al., 2011). The seismic response of this station is strongly affected by the presence of surface waves, generated within the basin, which cause significant amplifications at long periods both on vertical and horizontal components. A similar behavior can be observed for RTI station. Figure 6 shows the three components of the

recordings of the M=5.7, 1997 Umbria-Marche earthquake at RTI and their S-transform (Stockwell, 1996). Low-frequency late arrivals affect both vertical and horizontal components. The time-frequency domain plots show that late arrivals increase the spectral amplitudes over the frequency range 0.5 - 2 Hz. Since the EC8 schemes do not account for 2D-3D site effects, the presence of stations installed within alluvial basins contribute to the variability of residuals observed for classes C and D.

Figure 5 also shows the normalized residuals for two EC8 class A sites (red symbols), namely station PGL (Peglio) and SMT (Somplago Centrale). Strong under-estimation and over-estimations are observed for PGL (star symbol) and SMT (square symbol), respectively, that can be explained by the specific installation features. On one side, PGL is installed on weathered marly sandstones in correspondence of a ridge with average slope less than 30°. The under-estimation, occurring in the period range 0.2 - 0.3 s, shown by the normalized residuals, could be related to topographic effects (e.g., Géli et al, 1988; Paolucci, 2002), while the under-estimation at short periods could be related to the presence of weathered rock. On the other side, the strong over-estimations obtained for SMT are probably due to the installation of this station within a tunnel and the recording may be affected by destructive interference phenomena between the incident and surface-reflected waves (e.g. Tucker et al., 1984).

The normalized between-station errors relative to different classifications for the same station can be also compared. An example is shown in Figure 7a, where the errors obtained with EC8 and DiAlAl classifications are compared for the station CESV, classified as C in the EC8 scheme. From the HVSR curve (Figure 7b) the predominant period of CESV is 0.2s and the site is classified as CL-I (DiAlAl). This classification produces residuals larger than one τ for periods larger than 0.2 s, as well as the EC8 scheme. CL-I mainly includes rock and stiff sites, so the strong amplification occurring at CESV outside the period range defining class CL-I, leads to an under-estimation of the observations for periods larger than 0.2s. On the other hand, the strong peak at 0.5 s is evident for both classifications, indicating that this feature is distinctive of this station.

In conclusion, the analysis of the period dependent ε/τ ratio allows to identify those stations with remarkable differences with respect to the average response of their pertinence class.

6. Analysis of accelerometric stations in ITACA

To obtain sufficiently stable results and to summarize them in a synthetic format suitable to

be included into the station reports of the ITACA database, we considered the between-station errors only for the ITACA stations which recorded at least 6 earthquakes with magnitude larger than 3.5. As a tentative rule, a station is considered to present "anomalies", or distinctive features, in its seismic response if the normalized station error exceeds the ± 1τ dispersion band in a given period range. Furthermore, to guarantee that the results do not depend on the adopted classification, all four schemes introduced in this paper have been considered. Therefore, an anomalous seismic response of the station is detected if the between-station errors lie above or below the standard dispersion band at low, intermediate or long periods, for most of the adopted classification schemes. Results for the totality of the stations can be found in Paolucci and Bindi (2010), and in the single station reports downloadable from ITACA website. Typical examples of such results, roughly covering the identified anomalous types of response, are summarized in Figure 8. These and other examples will be briefly illustrated in the following paragraphs.

(a) ε/τ ratio *above the standard dispersion band at short periods (Figure 8a)*

This feature is represented by few cases of the dataset and is generally related to rock sites with a shallow weathered layer (< 10 m). A well-known case is Nocera Umbra (Central Italy), NCR/NCR2 (Rovelli et al., 2002), reported in Figure 8a. In this case, the presence of a buried "wedge" of weathered rock was supposed to be the main cause of the large peak of amplification at high-frequency. In the case the station is correctly classified as class E of the EC8, the errors are strongly reduced. Another interesting case of large amplifications in the short period range is the Caltagirone station (CLG), shown in Figure 9. The station is classified as class B, F-1 or CL VII according to different schemes and no large high-frequency amplification peaks are expected (Figure 3a). However, the large amplitudes at short periods observed for both components represent a distinctive feature of this station, probably related to a thin soil layer with shear wave velocity equal to 250 m/s, as shown in Figure 9.

(b) ε/τ ratio *above the standard dispersion band for short and long periods (Figure 8b)*

This feature could be associated to sites characterized by topographic irregularities. The clearest cases are Cascia (CSC, Fig. 8b) and Peglio (PGL, Figure 5) stations. Another example is station Naso (NAS), located on a rocky slope and characterized by large over-estimations, with a peak centred at 0.2 and 0.3 s on the horizontal and vertical components, respectively (Figure 10). Finally, several stations that recorded the 1980 Irpinia earthquake

(M 6.9) and its aftershocks show this feature. Further analyses on the within-station component of the error are necessary to verify the possibility that the between-event component of the error was not completely separated from the between-station component for these records.

(c) ε/τ ratio *above the standard dispersion band at long periods (Figure 8c)*

The ε/τ ratio being exceeded at long periods is one of the most interesting features of the database and it can be very often associated to the long-period basin-induced amplification effect, as illustrated in Figure 11, where all the plots refer to stations within alluvial basins. The amplification is related to the onset, propagation and reverberation of surface waves within the alluvial basins, as explained in more detail in this Special Issue by Smerzini et al. (2011), who made use of advanced 3D numerical approaches for seismic wave propagation in complex alluvial basins, and by Bindi et al. (2009b; 2011) and Cara et al (2011), who explored the in-field observations by temporary arrays installed inside the Gubbio, Norcia and Fucino basins.

(d) ε/τ ratio *below the standard dispersion band for short periods (Figure 8d).*

This feature is rather frequent among the stations of the ITACA database. Four out of them (CAMO, CAST, CMM, SEP) have recorded exclusively the 2002 Molise earthquake sequence, so that it may be argued that the between-event correction may not have completely removed the bias related to the specific characteristics of this seismic sequence (Bindi et al., 2009a). However, it is interesting to note that other stations belonging to this class, the results of which are shown in Figure 12, have the common characteristic of being located at the basement of massive buildings. Therefore, the de-amplification of short period spectral ordinates may be attributed to a kinematic interaction effect (see e.g. Stewart, 2000), as a result of high-frequency filtering of the ground motion by the embedded foundation.

(e) ε/τ ratio *below the standard dispersion band for short and long periods (Figure 8e)*.

Similarly to case (d), this feature is represented by four stations having recorded the Molise earthquake and by two stations, namely Spoleto Cantina (SPC) and Somplago Centrale Cunicolo (SMT), whose records are likely to be affected by interaction with the hosting structure. Furthermore SMT is an underground station located inside the tunnels of the

pumping stations of the Somplago power plant, so that this may be the cause of the broadband de-amplification of ground motion.

(f) ε/τ ratio *below the standard dispersion band for long periods (Figure 8f)*.

The only station clearly showing this feature is Monte Fiegni (MNF), which is located within a very complex geomorphological environment, at the border of an artificial basin.

Conclusions

Local site effects play an important role in determining the level of the ground shaking and its spatial variability. Ground motion predictive models should always include a description of these effects. However, since the available geological-geotechnical information about the site where the strong motion stations are installed is often poor, strong simplifications in modeling site effects is unavoidable when developing GMPEs. It follows that a significantly variability of the residuals between observations and predictions should be expected, both due to the complexity of the actual mechanisms generating site effects and to the simplified way in which they are accounted for in GMPEs.

In this work we analyzed the records of the Italian strong motion database (ITACA) with the aim of identifying the stations affected by peculiar site effects, which cannot be captured by simplified classification schemes. In particular, we considered four different classifications, two based on geological/geophysical information and two driven by recorded data. We used the ratio of the between-station error and the between-station standard deviation, to identify site effects not accounted for by the classification schemes.

This analysis allowed us to identify a broad set of cases for which complex geological conditions or station-structure interactions affect significantly the ground motion. In particular, we found two rather peculiar examples of such effects, namely:

- the long period amplification of ground motion affecting stations installed within alluvial closed-shape basins (Figure 11);

- the de-amplification of short period spectral ordinates for embedded stations, typically installed at the foundation level of massive structures (Figure 12).

While the first effect is well documented by earlier studies on stations of the Italian strong motion network, the second case deserves further studies. Moreover, it should be noted that, aside from the case depicted in Figure 8b, stations installed on topographic irregularities do not provide any systematic trend on results, at least within the dataset considered in this work.

Finally, this study confirms that classification schemes based on the site frequency (predominant or fundamental), derived from horizontal-to-vertical spectral ratios, do not improve predictions for stations installed in alluvial basins, since locally generated surface waves affect both horizontal and vertical components. Parameters complementary to the frequency, probably related to the geometry and/or thickness of the deposit, are necessary to properly classify stations with these characteristics.

Acknowledgements

We would like to thank J. Douglas and C. Di Alessandro for their valuable and constructive comments. This work was carried out in the framework of Project S4 "The Italian strong motion database", funded within the DPC-INGV 2007-09 Agreement, between the Italian Department of Civil Protection and the Istituto Nazionale di Geofisica e Vulcanologia.

References

Abrahamson, N. A., and R. R. Youngs (1992). A stable algorithm for regression analyses using the random effects model, Bull. Seismol. Soc. Am. 82, 505–510

Ambraseys, N.N., P. Smit, J. Douglas, B. Margaris, R. Sigbjörnsson, S. Ólafsson, P. Suhadolc and G. Costa (2004). Internet site for European strong-motion data, Bollettino di Geofisica e Applicata 45(3), 113-129.

Ambraseys, N.N., Douglas J., Sarma S., and P. Smit (2005) Equations for the estimation of strong ground motion from shallow earthquakes using data from Europe and the Middle East: Horizontal peak ground acceleration and spectral acceleration, Bull. Earthake. Engineering 3, 1-53

Al Atik L., N. Abrahamson, J. J. Bommer, F. Scherbaum, F. Cotton and N. Kuehn (2010). The Variability of Ground-Motion Prediction Models and Its Components Seismological Research Letters, 81, 794-801.

Barnaba C., Priolo E., Vuan A., Romanelli M. (2007). Site Effect of the Strong-Motion Site at Tolmezzo-Ambiesta Dam in Northeastern Italy, Bull Seismol Soc Am, vol. 97, 339-346.

Bindi D, F. Pacor, L. Luzi, R. Puglia, M. Massa, G.Ameri and R Paolucci (2010). Ground Motion Prediction Equations Derived from the Italian Strong Motion Data Base, submitted to Bull Seismol Soc Am

Bindi D, Luzi L, and F. Pacor (2009a). Interevent and Interstation Variability Computed for the Italian Accelerometric Archive (ITACA) Bull Seismol Soc Am; 99(4): 2471-2488. doi: 10.1785/0120080209

Bindi D., Parolai S.,Cara F., Di Giulio G., Ferretti G., Luzi L., Monachesi G., Pacor F. and Rovelli A. (2009b). Site amplifications observed in the Gubbio basin (Central Italy): hints for lateral propagation effects, Bull Seismol Soc Amer, 99, 2A, 741-760.

Bindi D, Luzi L, Pacor F, Franceschina G, and R. R. Castro (2006) Ground-Motion prediction from empirical attenuation relationships versus recorded data: the case of the 1997–1998 Umbria-Marches, Central Italy, Strong Motion Data Set, Bull Seismol Soc Am 96(3):984–1002. doi:10.1785/0120050102

Bindi D., L. Luzi, S. Parolai, D. Di Giacomo and F. Monachesi (2011) Site effects observed in alluvial basins: the case of Norcia (Central Italy). Submitted to Bull Earth. Eng, this Special Issue.

Boore, D.M. and G.M. Atkinson (2008). Ground-Motion Prediction Equations for the Average Horizontal Component of PGA, PGV, and 5%-Damped PSA at Spectral Periods between 0.01s and 10.0s, Earthquake Spectra, 24, 99-138.

Bragato, PL (2008). Limits for the Improvement of Ground-Motion Relations in Europe and the Middle East by Accounting for Site Effects, Bull Seismol Soc Am 98 (4), 2061-2065

Bragato PL (2009) Assessing regional and site-dependent variability of ground motions for ShakeMap implementation in Italy. Bulletin of the Seismological Society of America, 99(5):2950-2960, doi: 10.1785/0120090020Cara F., Di Giulio G., Cabinato G., Fagiani D. and G. Milana (2011) Seismic characterization and monitoring of Fucino basin. Submitted to Bull Earth. Eng, this Special Issue.

Castro, R.R., Pacor, F., Bindi D., Franceschina G., and Luzi, L. (2004), Site response of strong motion stations in the Umbria region, Central Italy, Bull. Seismol Soc. Am. 94, 576–590.

Comité Européen de Normalisation (CEN) (2004). Eurocode 8: Design of Structures for Earthquake Resistance—Part 1: General Rules, Seismic Actions and Rules for Buildings. Brussels: Comité Européen de Normalisation.

462 Cultrera, G., Rovelli, A., Mele, G., Azzara, R., Caserta, A., And Marra, F. (2003), Azimuth
463 dependent Amplification of Weak and Strong Ground Motions within a Fault Zone
464 (Nocera Umbra, Central Italy), J. Geophys. Res. 108 (B3), 2156,
465 doi:10.1029/2002JB001929.
466 Di Alessandro, C., L. F. Bonilla, A. Rovelli, O. Scotti (2008), Influence of site classification
467 on computing empirical ground-motion prediction equations in Italy, /EOS Trans. Am.
468 Geophys. Un., 89(53), Fall Meeting Suppl./, Abstract S12A-05.
469 Douglas, J. (2003). Earthquake ground motion estimation using strong-motion records: a
470 review of equations for the estimation of peak ground acceleration and response
471 spectral ordinates, Earth-Science Review 61 (1-2), 43-104.
472 Géli L, Bard P-Y, Jullien B. (1988). The effect of topography on earthquake ground motion:
473 a review and new results, Bull. Seism. Soc Am 78, 42– 63.
474
475 Lovati S., Bakavoli M.K.H., Massa M., Ferretti G., Pacor F., Paolucci R., Haghshenas E. and
476 Kamalian M. (2011). Estimation of topographical effects at Narni ridge (Central Italy):
477 comparisons between experimental results and numerical modeling. Submitted to Bull
478 Earth. Eng, this Special Issue.
479 Luzi L., M. Gallipoli, M.Mucciarelli D. Bindi and F. Pacor (2011). Testing of diffrent seismic
480 parameters for seismic parameters for site classification. Submitted to Bull Earth Eng,
481 this Special Issue.
482 Luzi L., Sabetta F., Hailemikael S., Bindi D., Pacor F., and F. Mele (2008). ITACA (ITalian
483 ACcelerometric Archive): a web portal for the dissemination of Italian strong motion
484 data. Seism Res Lett 79(5): 717–723. doi:10. 1785/gssrl.79.5
485 Luzi, L., D. Bindi, G. Franceschina, F. Pacor, and R. R. Castro (2005). Geotechnical Site
486 Characterisation in the Umbria Marche Area and Evaluation of Earthquake Site-
487 Response. Pure Appl. Geoph. 162, 2133–2161.
488 Massa M., Lovati S., D'Alema E., Ferretti G. and Bakavoli M. (2010). Experimental approach
489 for estimating seismic amplification effects at the top of a ridge and their implication
490 on ground motion predictions: the case of Narni (Central Italy), Bull. Seism. Soc.
491 Am., 100, 3020-3034.
492 Mucciarelli, M (2010). Identification of stations with possible significant interaction effects
493 with the hosting or surrounding structures, Deliverable D9, Appendix B,
494 http://esse4.mi.ingv.it

Pacor F., Bindi D., Luzi L., Parolai S., Marzorati S. and Monachesi G. (2007). Characteristics of strong ground motion data recorded in the Gubbio sedimentary basin (Central Italy), Bull. Earth. Eng. 5, 27-43

Paolucci R. (2002) Amplification of earthquake ground motion by steep topographic irregularities, Earthquake Engineering & Structural Dynamics, 31: 1831-1853.

Paolucci R. and D. Bindi (2010). Analysis of strong motion records for identification of stations with distinctive seismic response. Appendix A of Deliverable D9 - Project S4. Available at the web site http://esse4.mi.ingv.it.

Rovelli, A., A. Caserta, F. Marra, and V. Ruggiero (2002). Can seismic waves be trapped inside an inactive fault zone? The case study of Nocera Umbra, central Italy, Bull. Seismol. Soc. Am. 92, 2217–2232.

Sabetta F, and A. Pugliese (1996) Estimation of response spectra and simulation of non-stationary earthquake ground motions. Bull Seismol Soc Am 86(2):337–352

Sabetta F. and A. Pugliese (1987). Attenuation of peak horizontal acceleration and velocity from Italian strong-motion records, Bull. Seis. Soc. of Am., 77(5):1491-1513

Smerzini C., M. Stupazzini and R. Paolucci (2011) Comparison of 3D, 2D and 1D numerical approaches to predict long period earthquake ground motion in the Gubbio plain, Central Italy. Submitted to Bull Earth. Eng, this Special Issue.

Stewart J (2000) Variations between foundation-level and free-field earthquake ground motions. Earthquake Spectra 16:511–532.

Stockwell, R. G., L. Mansinha, and R. P. Lowe (1996). Localization of the complex spectrum: the S transform. IEEE Trans. Signal Process., Vol. 44, pp. 998–1001.

Strasser, F. O., N. A. Abrahamson, and J. J. Bommer (2009). Sigma: Issues, insights, and challenges. Seismological Research Letters 80,41–56.

Toro, G.R., N.A. Abrahamson and J.F. Schneider, (1997) Model of strong ground motions from earthquakes in Central and Eastern North America: best estimates and uncertainties. Seismological Research Letters, 68, 1, pp. 41–57

Tucker, B. E., J. L. King, D. Hatzefeld and I. L. Nersesov (1984). Observations of hard-rock site effects, Bull. Seism. Soc. Am. 74, 121-136.

Zhao O. X., J. Zhang , A. Asano, Y. Ohno, T. Oouchi, T. Takahashi, H. Ogawa, K. Irikura, H. K. Thio, P. G. Somerville, Y. Fukushima, and Y. Fukushima (2006). Attenuation Relations of Strong Ground Motion in Japan Using Site Classification Based on Predominant Period, Bull. Seism. Soc. Am 96, 898 - 913.

FIGURE CAPTIONS

Figure 1. Left: median spectral acceleration in [m/s^2] at 0.1 s predicted (Bindi et al. 2010) for a magnitude 4.25 earthquake (black) and observations for two different earthquakes (circles) with similar magnitude. The median values plus the between-event error of the two earthquakes are shown as coloured lines. Right: median spectral acceleration (black) at 1.75 s predicted for a magnitude 5.5 earthquake and observations at three different stations (GBP, CLC and AVZ) of different earthquakes with similar magnitudes (circles). The median values plus the between-station (ε) and within-station (η) errors at the three stations are indicated as well (see also equation 1).

Figure 2. Magnitude versus distance scatter plot for different site classification schemes. Top: SP classification (left); EC8 classification (right). Bottom: LuAl classification (left); DiAlAl classification (right). Different colors indicate different classes in each frame.

Figure 3. Site coefficients obtained for the different classification schemes described in Table 1. Different symbols correspond to different classes, as shown in each frame: a) horizontal components, b) vertical component

Figure 4 Inter station errors. The circles are color coded accordingly to the EC8 classes (colors from red to blue correspond to classes A through E, respectively). Top: 0.1s (left) and 0.25 s (right). Bottom: 1s (left) and 2 s (right).

Figure 5 (Left) Period dependence of the between-station residuals normalized to the between-station standard deviation for some stations (EC8 classification). Blue indicate station classified as C; red as A. Circle: RTI; triangle: GBP; diamond: PGL; square: SMT; (Right) vertical component

Figure 6. Top: recordings of the Umbria-Marche mainshock (Mw=5.7) at station RTI (Rieti, epicentral distance 66 km). The time series over the three components are filtered over the frequency band 0.1-25 Hz. Bottom: time-frequency images computed by applying the S-transform (Stockwell, 2006). The S-transforms are normalized to the maximum estimated over the three components and a common logarithmic color scale from -4 (blue) to 0 (red) is used.

Figure 7. Cesi Valle (CSV) station. a) Station residuals normalized to the between-station standard deviation for station CESV and different site classification schemes. Results for geoH component are shown in blue (DiAlAl) and gray (EC8). The results for the vertical component obtained considering EC8 are shown in red. b) Horizontal to Vertical ratio of response spectra computed from accelerograms recorded at station CESV (black lines). The mean ± 1 standard deviations are shown as red lines. Left: ratio between the East-West (EW) and vertical (Z) components; right: ratio between the North-South (NS) and vertical components.

Figure 8 Types of anomalous responses recognized in the ITACA database. Top: spectral ordinates above the standard dispersion band of GMPEs a) short periods; b) both short and long periods c) long periods.
Bottom: Spectral ordinates below the standard dispersion band of GMPEs d) short period e) both short and long periods f) long periods

Figure 9 Caltagirone station (CLG). Normalized error distribution for: a) horizontal component; b) vertical component; c) Vs profile estimated with surface waves (ITACA report, 2010)

Figure 10 Naso station (NAS). Normalized error distribution for: a) horizontal component; b) vertical component. the site is classified as rock on the base of geological information.

Figure 11 Stations Gubbio Piana (GBP), Rieti (RTI), Norcia (NCR), Bevagna (BGV), and Castelnuovo Assisi (CSA) are located on alluvial deposit within typical basins of central Italy, having tectonic origin. Catania (CAT) is installed on the alluvial plain of Catania city (southern Italy) characterized by very soft deposits.

Figure 12 Stations Antrodoco (ANT), Avezzano (AVZ) and Fiamignano (FMG), installed inside buildings.

TABLE

Table 1: Site classification schemes adopted in this study.

SP87 (Sabetta and Pugliese; 1987)	**0**	**1**	**2**				
Geological description	>rock site	Shallow alluvium	Deep alluvium				
EC8 (2004)	**A**	**B**	**C**	**D**	**E**		
Vs,30 (m/s)	>800	360–800	180–360	< 180	shallow soil layer with V_{s30} of class C or D and thickness varying between 5 and 20m. overlaying stiffer material (V_{s30}>800 m/s)		
DiAlAl (Di Alessandro et al.; 2008)	**CL-I**	**CL-II**	**CL-III**	**CL-IV**	**CL-V**	**CL-VI**	**CL-VII**
Predominant period Tg (s)	< 0.2	0.2-0.4	0.4-0.6	>0.6	Tg not identifiable (flat H/V and amplitude < 2)	broad amplification/ multiple peaks @ Tg > 0.2 sec.	Tg not identifiable (multiple peaks over entire period range)
LuAl (Luzi et al.; 2011)	**F-0**	**F-1**	**F-2**	**F-3**	**F-4**		
Fundamental frequency (Hz)	HVSR amplitude < 2	1.1±0.5	3.5±0.8	6.3±1	HVSR with Broad Band amplification		

Table 2: Number of stations, earthquakes and records used for each classification scheme used in this study. The number of recordings for each class (Table 1) is shown in the last column between parentheses.

Classification	# stations	# earthquakes	# records
SP	225	339	1181 (503;352;326)
EC8	391	360	1616 (698;463;328;46;81)
LuAl	180	329	1099 (241;301;196;200;161)
DiAlAl	178	303	939(225;163;132;155;87;66;111)

Figures

Click here to download line figure: figureBindiRev1_v1.doc

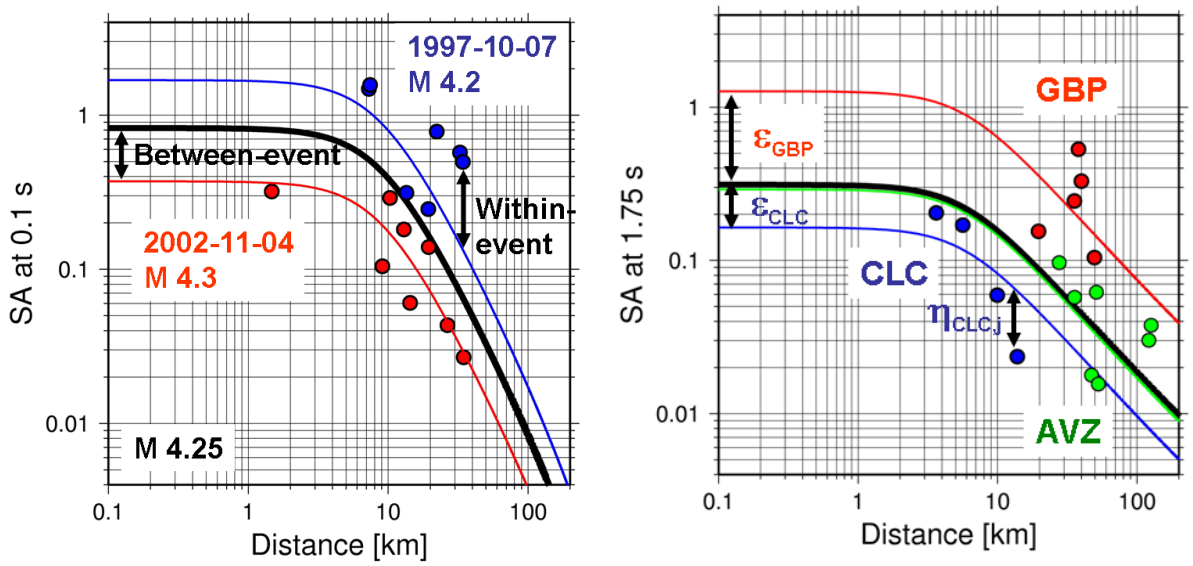

Figure 1. Left: median spectral acceleration in [m/s^2] at 0.1 s predicted (Bindi et al. 2010) for a magnitude 4.25 earthquake (black) and observations for two different earthquakes (circles) with similar magnitude. The median values plus the between-event error of the two earthquakes are shown as coloured lines. Right: median spectral acceleration (black) at 1.75 s predicted for a magnitude 5.5 earthquake and observations at three different stations (GBP, CLC and AVZ) of different earthquakes with similar magnitudes (circles). The median values plus the between-station (ε) and within-station (η) errors at the three stations are indicated as well (see also equation 1).

.

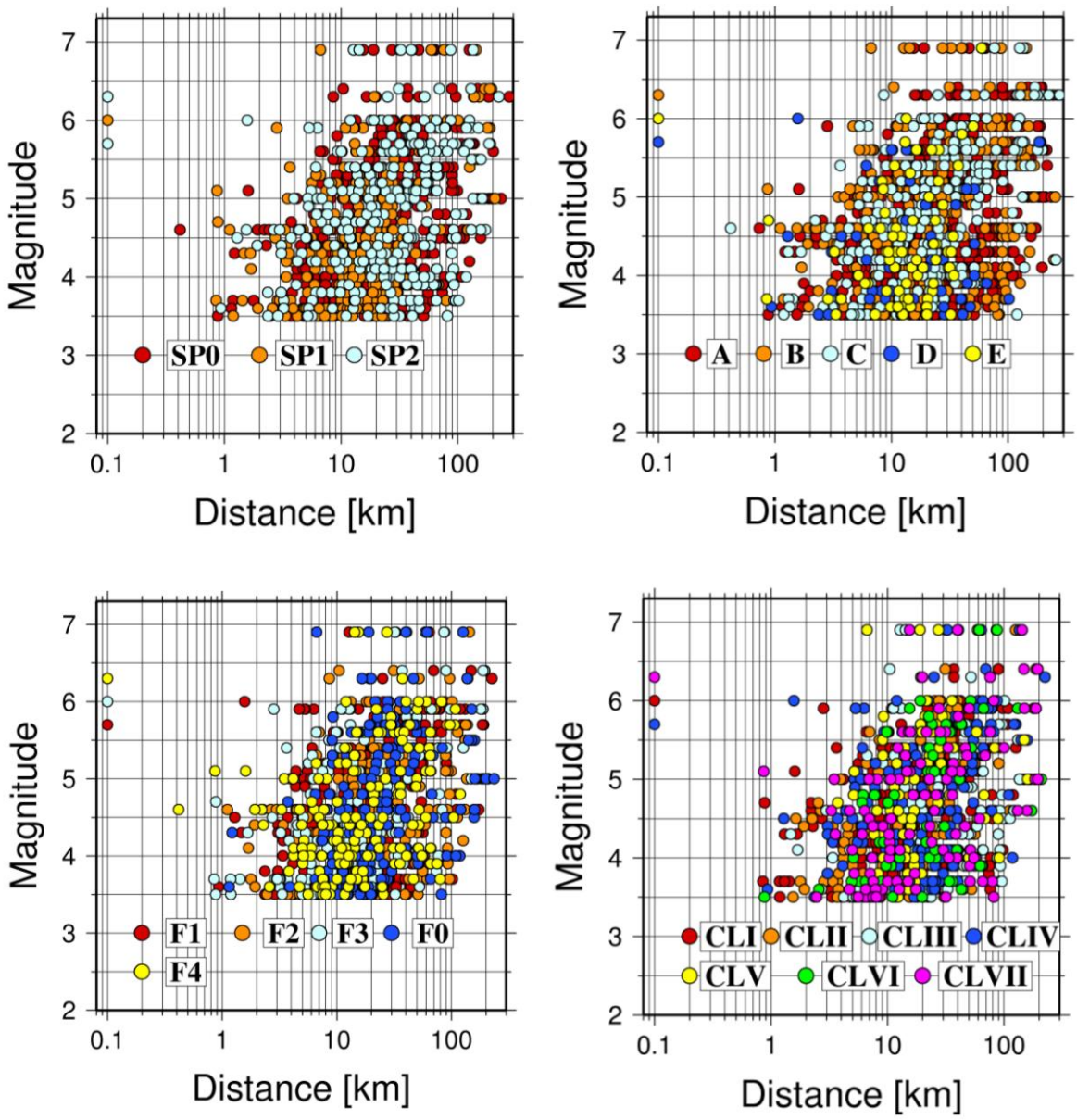

Figure 2. Magnitude versus distance scatter plot for different site classification schemes. Top: SP classification (left); EC8 classification (right). Bottom: LuAl classification (left); DiAlAl classification (right). Different colors indicate different classes in each frame.

a)

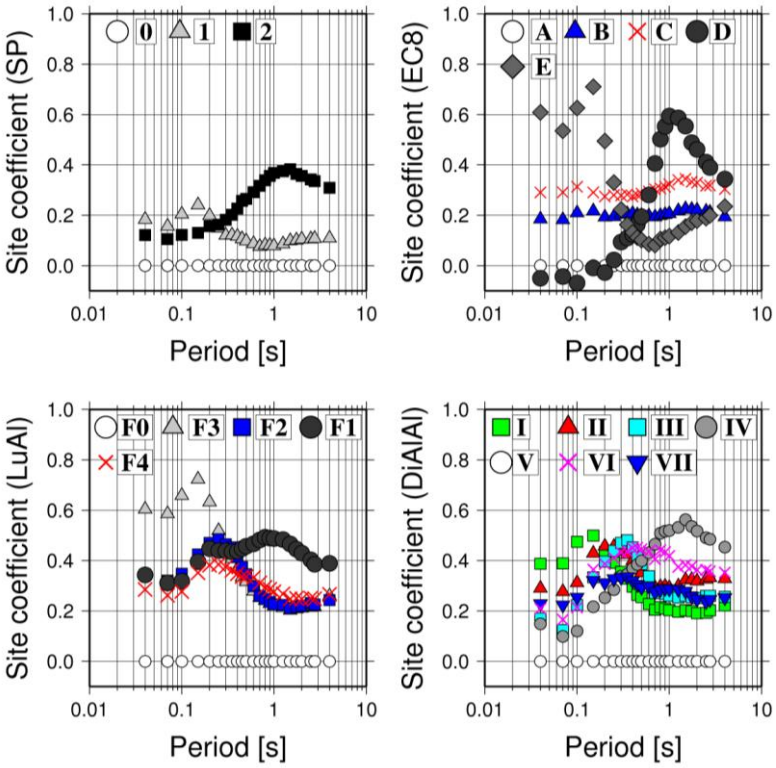

b)

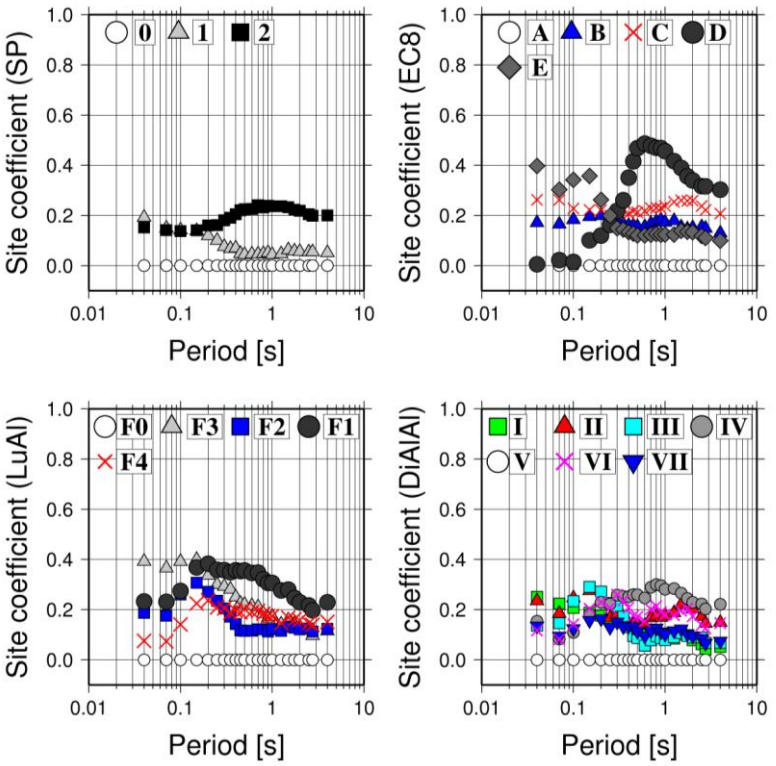

Figure 3. Site coefficients obtained for the different classification schemes described in Table 1. Different symbols correspond to different classes, as shown in each frame: a) horizontal components, b) vertical component.

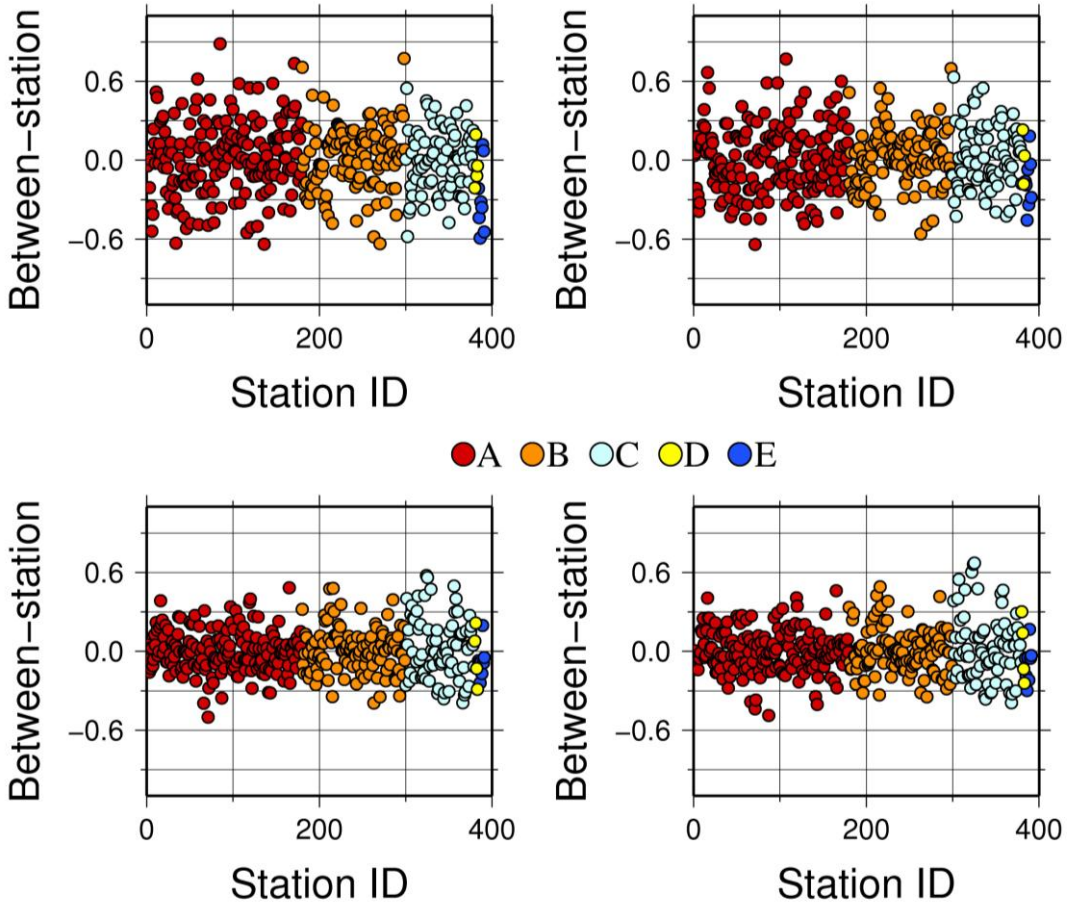

Figure 4 Between-station errors. The circles are color coded accordingly to the EC8 classes (colors from red to blue correspond to classes A through E, respectively). Top: 0.1s (left) and 0.25 s (right). Bottom: 1s (left) and 2 s (right).

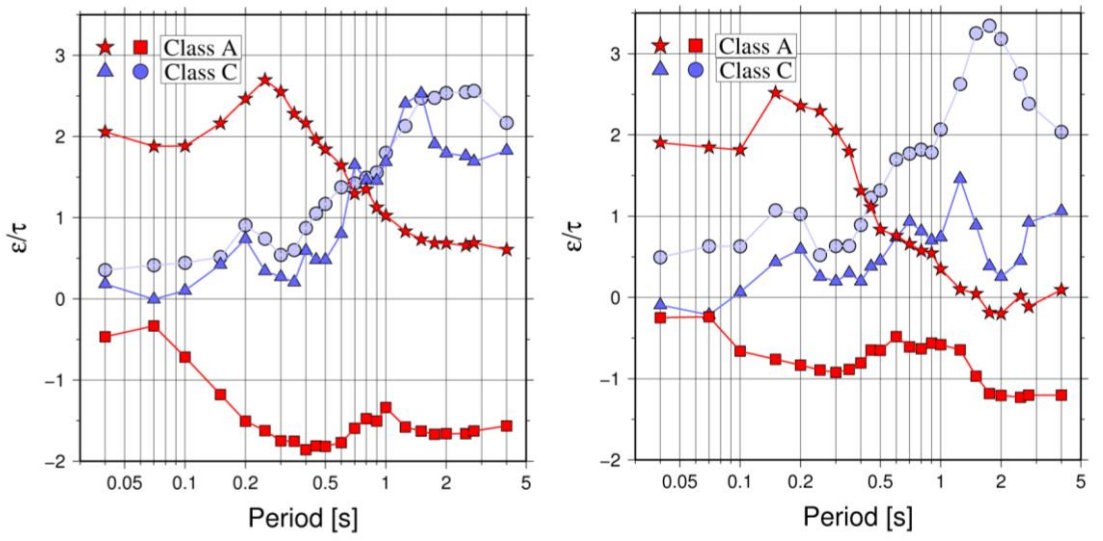

Figure 5. (Left) Period dependence of the between-station residuals normalized to the between-station standard deviation for some stations (EC8 classification). Blue indicate station classified as C; red as A. Circle: RTI; triangle: GBP; star: PGL; square: SMT; (Right) vertical component.

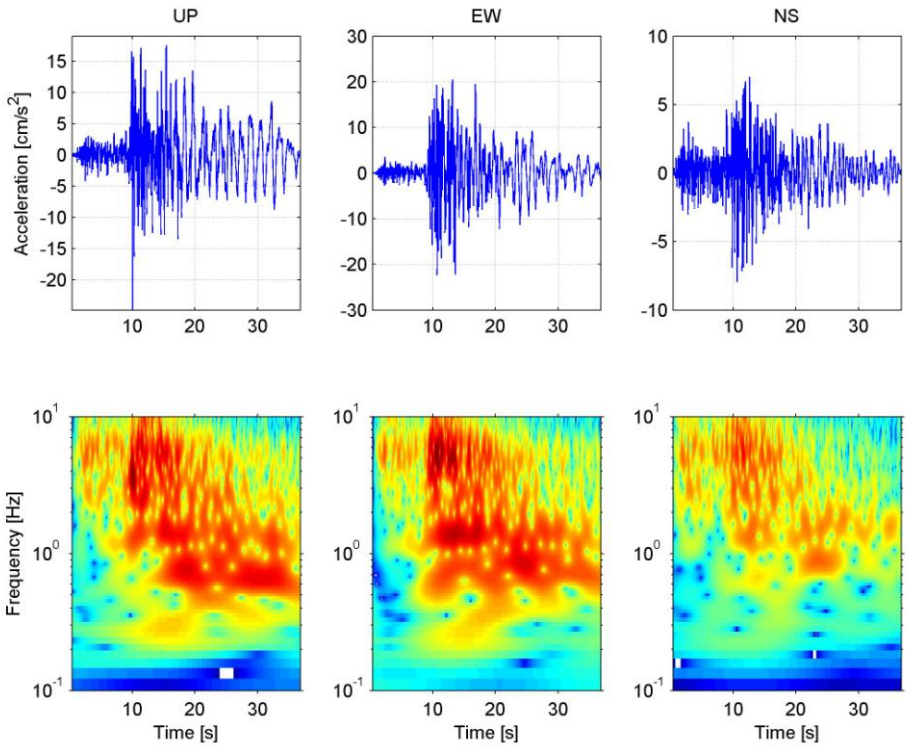

Figure 6. Top: recordings of the Umbria-Marche mainshock (Mw=5.7) at station RTI (Rieti, epicentral distance 66 km). The time series over the three components are filtered over the frequency band 0.1-25 Hz. Bottom: time-frequency images computed by applying the S-transform (Stockwell, 2006). The S-transforms are normalized to the maximum estimated over the three components and a common logarithmic color scale from -4 (blue) to 0 (red) is used.

a)

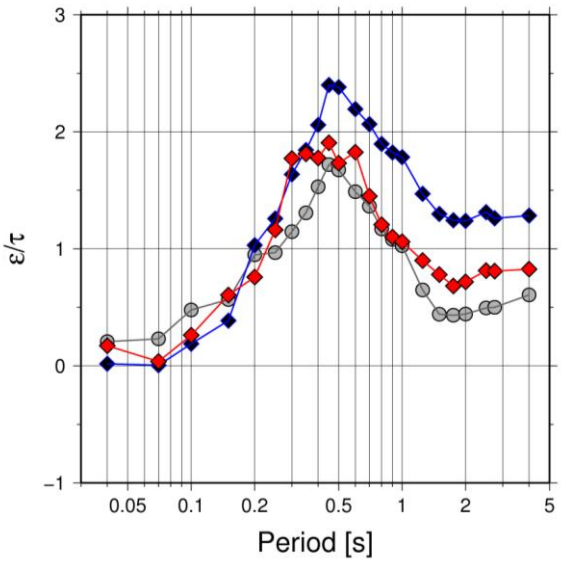

b)

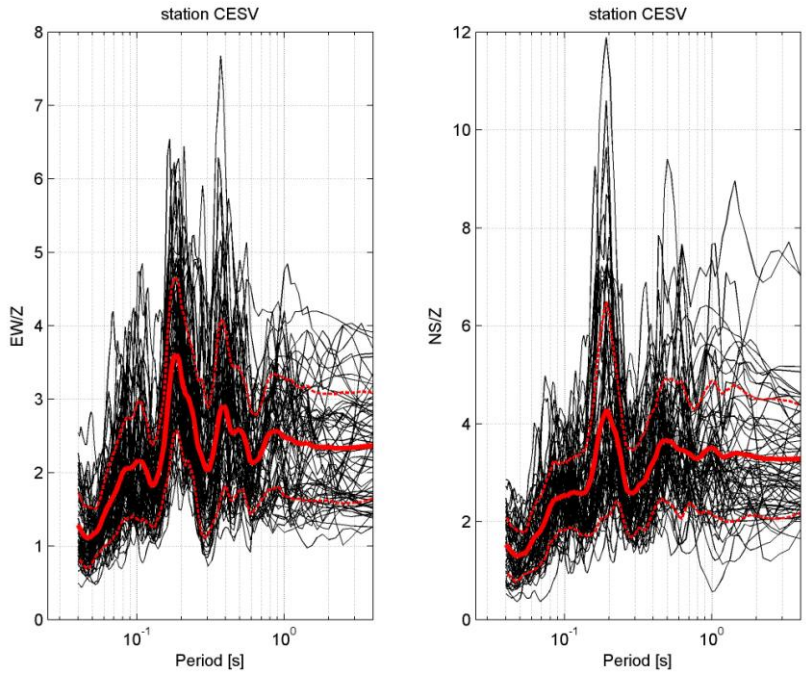

Figure 7. Cesi Valle (CSV) station. a) Station residuals normalized to the between-station standard deviation for station CESV and different site classification schemes. Results for geoH component are shown in blue (DiAlAl) and gray (EC8). The results for the vertical component obtained considering EC8 are shown in red. b) Horizontal to Vertical ratio of response spectra computed from accelerograms recorded at station CESV (black lines). The mean ± 1 standard deviations are shown as red lines. Left: ratio between the East-West (EW) and vertical (Z) components; right: ratio between the North-South (NS) and vertical components.

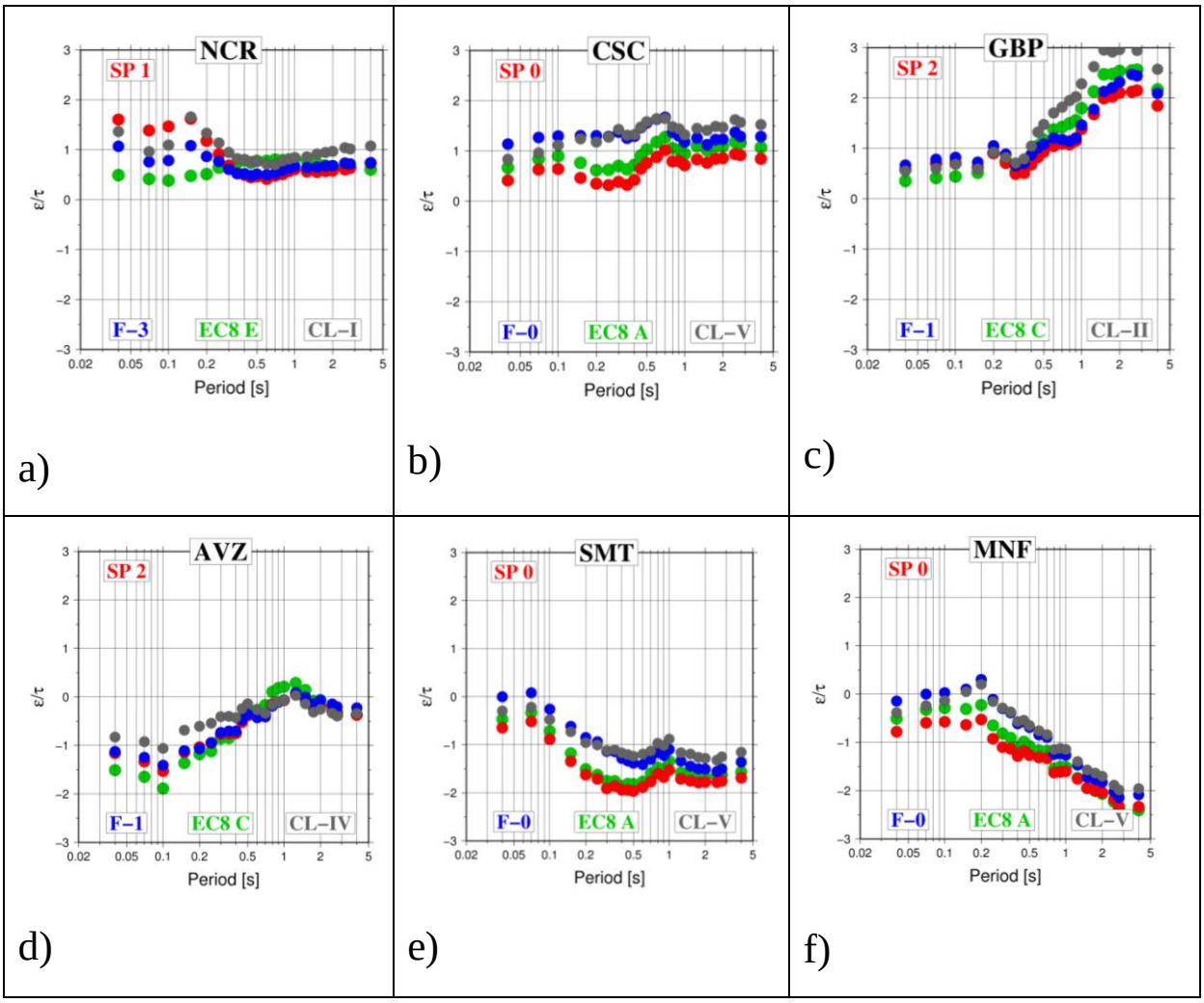

Figure 8 Types of anomalous responses recognized in the ITACA database. Top: spectral ordinates above the standard dispersion band of GMPEs a) short periods; b) both short and long periods c) long periods.

Bottom: Spectral ordinates below the standard dispersion band of GMPEs d) short period e) both short and long periods f) long periods

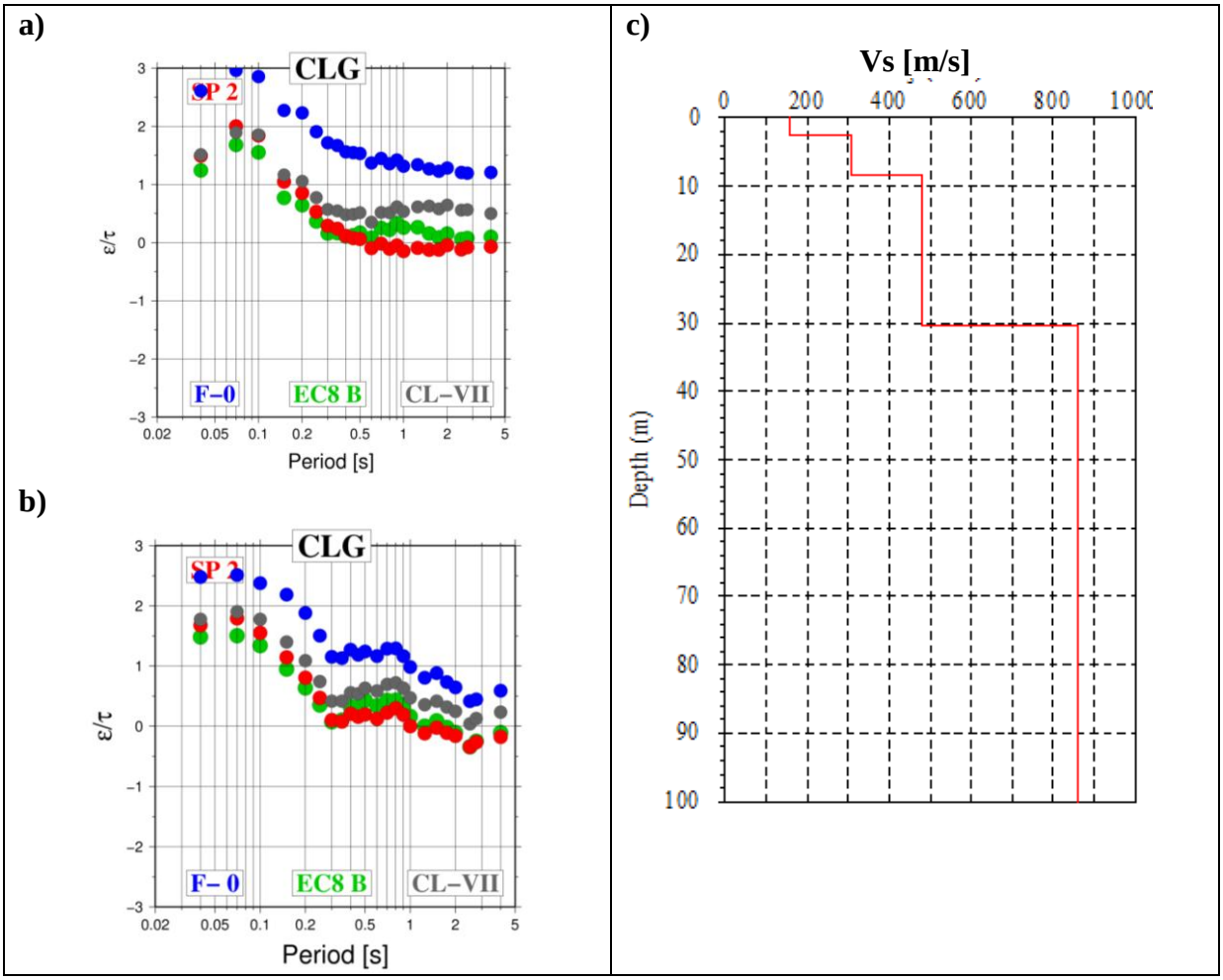

Figure 9 Caltagirone station (CLG). Normalized error distribution for: a) horizontal component; b) vertical component; c) Vs profile estimated with surface waves (ITACA report, 2010)

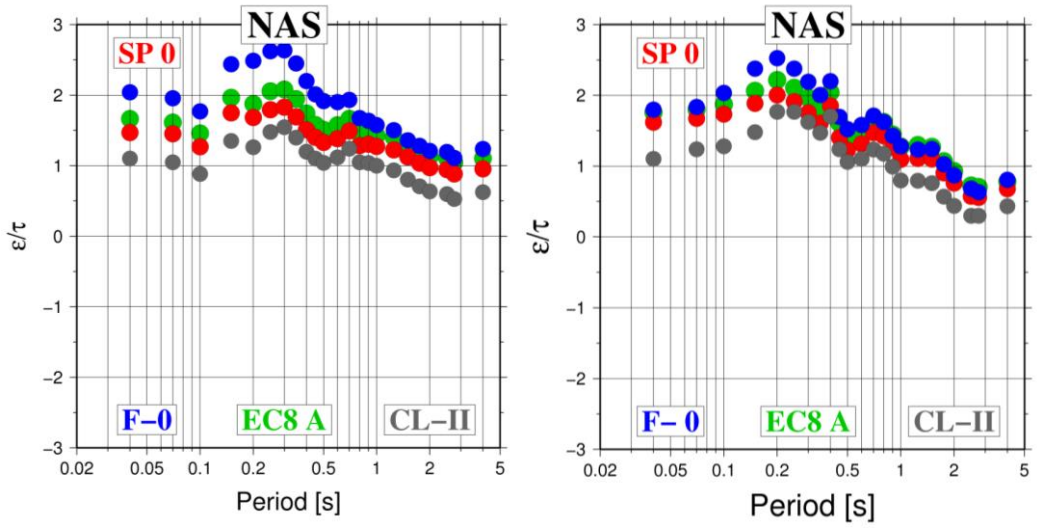

Figure 10 Naso station (NAS). Normalized error distribution for: a) horizontal component; b) vertical component. The site is classified as rock on the base of geological information.

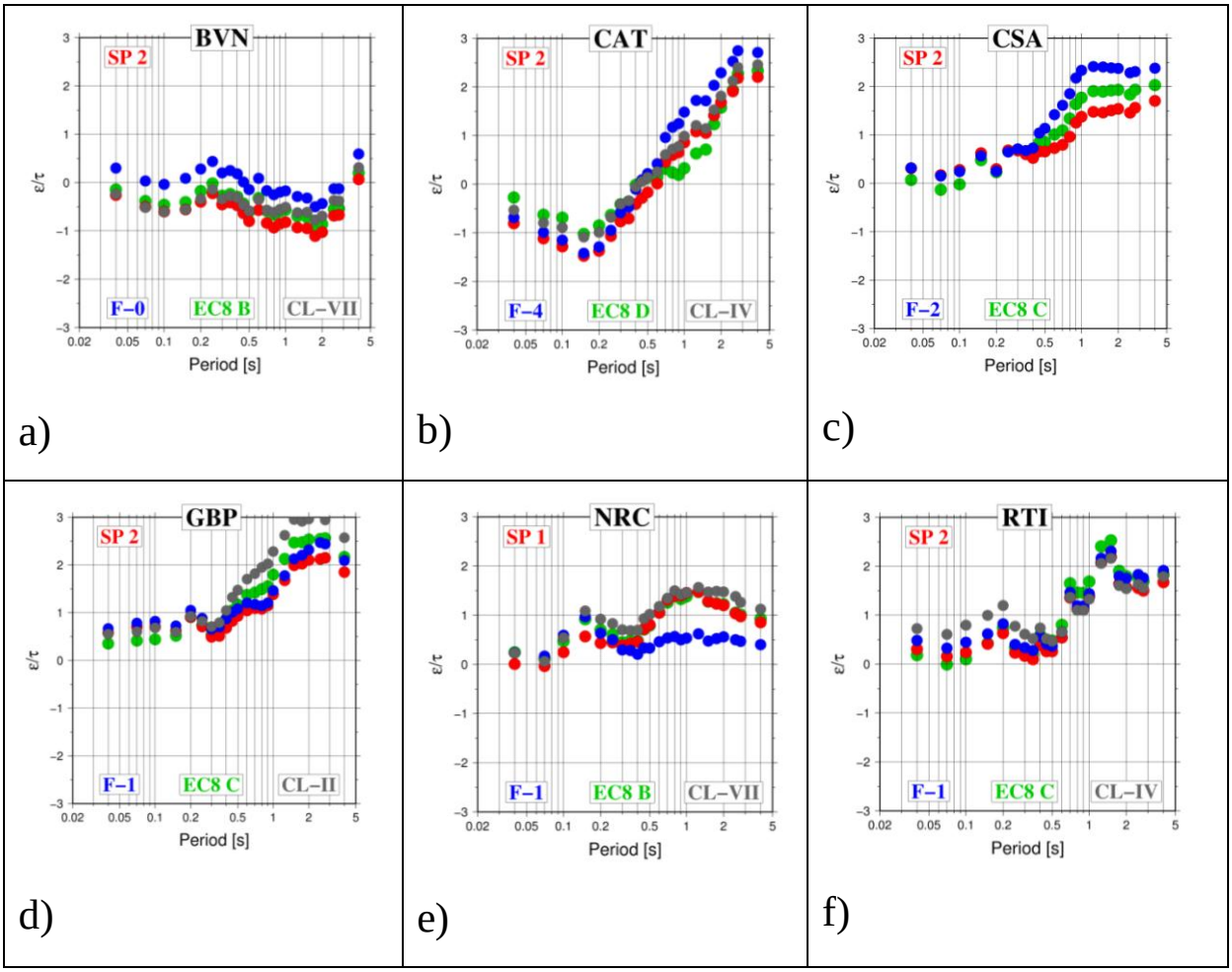

Figure 11 Stations Gubbio Piana (GBP), Rieti (RTI), Norcia (NCR), Bevagna (BGV), and Castelnuovo Assisi (CSA) are located on alluvial deposit within typical basins of central Italy, having tectonic origin. Catania (CAT) is installed on the alluvial plain of Catania city (southern Italy) characterized by very soft deposits.

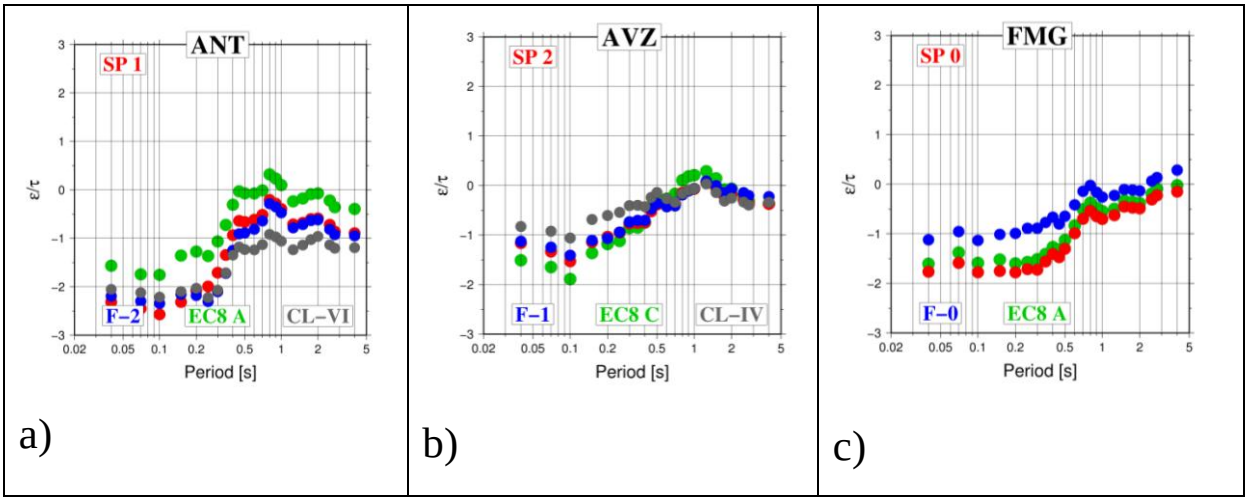

Figure 12 Stations Antrodoco (ANT), Avezzano (AVZ) and Fiamignano (FMG), installed inside buildings.